SLC26A9 is a Cl^- channel regulated by the WNK kinases

Michael R. Dorwart[1], Nikolay Shcheynikov[1], Youxue Wang[1], Steve Stippec[2] and Shmuel Muallem[1]

Department of [1]Physiology and [2]Pharmacology, University of Texas Southwestern Medical Center at Dallas, Dallas, TX 75390-9040, USA

SLC26A9 is a member of the SLC26 family of anion transporters, which is expressed at high levels in airway and gastric surface epithelial cells. The transport properties and regulation of SLC26A9, and thus its physiological function, are not known. Here we report that SLC26A9 is a highly selective Cl^- channel with minimal OH^-/HCO_3^- permeability that is regulated by the WNK kinases. Expression in *Xenopus* oocytes and simultaneous measurement of membrane potential or current, intracellular pH (pH_i) and intracellular Cl^- (Cl^-_i) revealed that expression of SLC26A9 resulted in a large Cl^- current. SLC26A9 displays a selectivity sequence of $I^- > Br^- > NO_3^- > Cl^- > Glu^-$, but it conducts $Br^- > Cl^- > I^- > NO_3^- > Glu^-$, with NO_3^- and I^- inhibiting the Cl^- conductance. Similarly, expression of SLC26A9 in HEK cells resulted in a large Cl^- current. Although detectable, OH^- and HCO_3^- fluxes in oocytes expressing SLC26A9 were very small. Moreover, HCO_3^- had no discernable effect on the Cl^- current, the reversal potential in the presence or absence of Cl^-_o and, importantly, HCO_3^- had no effect on Cl^- fluxes. These findings indicate that SLC26A9 is a Cl^- channel with minimal OH^-/HCO_3^- permeability. Co-expression of SLC26A9 with the WNK kinases WNK1, WNK3 or WNK4 inhibited SLC26A9 activity, and the inhibition was independent of WNK kinase activity. Immunolocalization in oocytes and cell surface biotinylation in HEK cells indicated that the WNK-mediated inhibition of SLC26A9 activity is caused by reduced SLC26A9 surface expression. Expression of SLC26A9 in the airway and the response of the WNKs to homeostatic stress raise the possibility that SLC26A9 serves to mediate the response of the airway to stress.

(Received 3 May 2007; accepted after revision 1 August 2007; first published online 2 August 2007)
Corresponding author S. Muallem: Department of Physiology, University of Texas Southwestern Medical Center at Dallas, Dallas, TX 75390-9040, USA. Email: shmuel.muallem@utsouthwestern.edu

Cl^- absorption and HCO_3^- secretion are vital functions of epithelia. In most epithelia, like the airway (Wine, 2006), pancreas (Steward *et al.* 2005), salivary glands (Melvin *et al.* 2005), intestine (Binder *et al.* 2005) and the reproductive system (Chan *et al.* 2006) Cl^- absorption and HCO_3^- secretion are dependent on the function of the cystic fibrosis transmembrane conductance regulator (CFTR). Although CFTR functions as a Cl^- channel that can also conduct some HCO_3^- (Poulsen *et al.* 1994; Linsdell *et al.* 1997), recent work revealed that CFTR is regulated by extracellular Cl^- (Cl^-_o) (Shcheynikov *et al.* 2004; Wright *et al.* 2004) and is not likely to mediate most of the Cl^- absorption and HCO_3^- secretion by secretory epithelia (Wang *et al.* 2003).

HCO_3^--secreting epithelia also express coupled Cl^-–HCO_3^- exchangers at the luminal membrane. It is now clear that the luminal Cl^-–HCO_3^- exchangers are members of the SLC26 family of transporters (SLC26Ts). The family consists of 10 genes, most of which have several splice variants (Mount & Romero, 2004). Mutations in several members of the family are associated with human diseases such as diastrophic dysplasia (SLC26A2) (Superti-Furga *et al.* 1996), congenital Cl^- diarrhoea (SLC26A3) (Makela *et al.* 2002), Pendred syndrome (SLC26A4) (Everett *et al.* 1997) as well as non-syndromic forms of deafness (SLC26A5) (Liu *et al.* 2003). The Cl^- and HCO_3^- transport properties are specific to each member of the family. SLC26A1 and SLC26A2 function primarily as SO_4^{2-} transporters (Mount & Romero, 2004), while SLC26A3 functions as a coupled $2Cl^-$–$1HCO_3^-$ exchanger (Ko *et al.* 2002; Shcheynikov *et al.* 2006). SLC26A4 transports I^- (Dossena *et al.* 2006) and also mediates Cl^-–HCO_3^- exchange (Wall, 2005), while SLC26A6 functions a coupled $1Cl^-$–$2HCO_3^-$ exchanger (Xie *et al.* 2002; Shcheynikov *et al.* 2006) and SLC26A7 functions as a pH_i-regulated Cl^- channel (Kim *et al.* 2005).

Another member of the family that is expressed at high levels primarily in the airway (Lohi *et al.* 2002) and gastric surface epithelial cells (J. Xu *et al.* 2005) is SLC26A9. SLC26A9 was reported to function as a Cl^-–HCO_3^- exchanger that is inhibited by NH_4^+ (J. Xu *et al.* 2005).

M. R. Dorwart and N. Shcheynikov contributed equally to this work.

DOI: 10.1113/jphysiol.2007.135855

The mRNA level of SLC26A9 is up-regulated in the gastric mucosa of mice infected with *Helicobacter pylori* (Henriksnas *et al.* 2006). Accordingly, it was proposed that SLC26A9 in gastric surface epithelial cells mediates the HCO_3^- secretion needed for protection of the gastric mucosa against injury by gastric acid (J. Xu *et al.* 2005; Henriksnas *et al.* 2006). To fulfil this task SLC26A9 should be a potent HCO_3^- transporter and its HCO_3^- transport properties should be similar to the HCO_3^- transport properties of surface epithelial cells. This should include DIDS-sensitive Cl^--dependent electroneutral and Cl^--independent conductive pathways, both of which were described in gastric surface epithelia (Curci *et al.* 1994; Allen & Flemstrom, 2005).

A major regulator of epithelial Na^+, K^+ and Cl^- transport are the WNK (with no lysine) family of protein kinases, which were first discovered in a nested PCR screen to identify novel members of the MAP kinase family (Xu *et al.* 2000). The WNK name was given to these kinases because the highly conserved catalytic lysine in β strand 3 of the kinase domain is missing in the WNKs. However, it was later shown (Xu *et al.* 2002), and confirmed by the crystal structure of the WNK1 kinase domain (Min *et al.* 2004), that the catalytic lysine is contributed by β strand 2 of the kinase domain. The WNK family consists of four members that show about 45% overall identity with about 85% identity in the kinase domain (Gamba, 2005; Xie *et al.* 2006). To date, only WNK1, 3 and 4 have been cloned and their activity tested. The physiological role of the WNKs became evident with the discovery that mutations in WNK1 and WNK4 are linked to the familial hyperkalaemic hypertension disorder pseudohypoaldosteronism type II (PHAII) (Wilson *et al.* 2001). Several subsequent studies revealed that the WNKs regulate key transporters at the apical and basolateral membrane of selective renal tubular segments (reviewed in Gamba, 2005; Kahle *et al.* 2005; Subramanya *et al.* 2006; Xie *et al.* 2006). Thus, the WNKs regulate the Na^+–Cl^- cotransporter NCC1 (Kahle *et al.* 2005; Subramanya *et al.* 2006), the K^+–Cl^- cotransporters KCC1 and KCC2 (de Los Heros *et al.* 2006), the Na^+–K^+–$2Cl^-$ cotransporters NKCC1 (Anselmo *et al.* 2006) and NKCC2 (Rinehart *et al.* 2005), the K^+ channel ROMK (Lazrak *et al.* 2006; Leng *et al.* 2006) and the epithelial Na^+ channel ENaC (Naray-Fejes-Toth *et al.* 2004; B. E. Xu *et al.* 2005). In addition, WNK4, but not WNK1, inhibits SLC26A6, but not SLC26A4 (Kahle *et al.* 2004). Invariably, the WNKs regulate the transporters by modulating their surface expression, rather than affecting their transport properties (see Gamba, 2005; Kahle *et al.* 2005; Subramanya *et al.* 2006; Xie *et al.* 2006).

Another prominent regulator of the SLC26Ts is CFTR. In a previous work we showed that CFTR regulates the activity of mouse slc26a3, human SLC26A4 and mouse slc26a6 (Ko *et al.* 2002). This regulation is facilitated by interaction of CFTR and the SLC26Ts with PDZ domain-containing scaffolding proteins and is mediated by interaction of the CFTR R-domain and the SLC26Ts STAS domain (Ko *et al.* 2004).

In the present work we show that SLC26A9 is a Cl^- channel with minimal OH^-/HCO_3^- permeability. The channel displays a selectivity order of $I^- > Br^- > NO_3^- > Cl^- > Glu^-$, but it conducts $Br^- > Cl^- > I^- > NO_3^- > Glu^-$, with NO_3^- and I^- inhibiting Cl^- conductance by SLC26A9. These properties do not support a role of SLC26A9 in HCO_3^- transport. We also show here that WNK1, WNK3 and WNK4 inhibit SLC26A9 expressed in *Xenopus* oocytes or HEK cells by reducing its surface expression. The potential significance of these findings to epithelial transport, cystic fibrosis and stress sensing is discussed.

Methods

Clones

The SLC26A9 cDNA was generously provided by Dr Juha Kere (Karolinska Institutet, Sweden), which was subcloned into the *Sal* I and *Xho* I restriction sites of the HA-pCMV vector (Clontech). Two SLC26A9 isoforms can be found in the Nucleotide database, and all the studies presented here have used variant 1 (gi:20336286). Upon sequencing the open reading frame a sequence variation in SLC26A9 (K147E) was found that has no functional significance (data not shown) and thus may represent polymorphism of SLC26A9. A double-tagged SLC26A9 construct was made by inserting a myc tag between T787 and L788 of the HA-tagged construct described above, thus preserving the PDZ ligand at the C-terminus. Full length *Rattus norvegicus* WNK1, *Mus musculus* WNK4 kinase constructs in the pCMV5 vector and *Homo sapiens* WNK3 in the pCMV6 vector were generous gifts from Dr Melanie Cobb (UT Southwestern Medical Center, Dallas, TX, USA), and are described in detail elsewhere (Xu *et al.* 2000, personal communication). The WNK1, WNK3 and WNK4 cDNAs were shuttled into the T7TS expression vector for cRNA production using standard methods. cRNA was produced using the mMESSAGE mMACHINE following the manufacturer's guidelines (Ambion). The WNK3(K159M) and WNK4(K183M) kinase-dead mutant constructs and the WNK3(1–410) kinase domain in the T7TS construct were generated using the QuickChange Site-Directed Mutagenesis Kit (Stratagene) following the manufacturer's guidelines.

Total and surface expression in HEK cells and *Xenopus* oocytes

Expression of SLC26A9 was assayed by Western blots and surface expression by biotinylation (HEK cells) or immunolocalization (oocytes).

Biotinylation assay

The biotinylation assay was similar to that previously described (Kim *et al.* 2006). In brief, HEK cells were cultured in Dulbecco's Modified Eagle's Medium (DMEM) containing 10% fetal bovine serum (FBS). Transfections were performed with Lipofectamine Plus following the manufacturer guidelines, and the cells were used 36–48 h post transfection. Sulfo-NHE-ss-Biotin in PBS was added to cells transfected with empty vector, SLC26A9, or SLC26A9 and the WNK kinases, and the cells were incubated for 30 min at 0°C. Free biotin was quenched and washed with 1% bovine serum albumin (BSA) in PBS. The cells were used to prepare microsomes by homogenization in buffer containing (mM): 250 sucrose, 10 Hepes, 1 EDTA, 1 DTT, 0.2 PMSF. After centrifugation for 3 min at 1000 r.p.m. in an Eppendorf centrifuge, the supernatants were centrifuged for 20 min at 18 000 r.p.m. The microsomal pellet was dissolved in lysis buffer containing (mM): 20 Tris, pH 8.0, 137 NaCl, 5 NaEDTA, 5 NaEGTA, 10% glycerol, 0.5% Triton X-100, 0.2 PMSF, 50 NaF, 20 benzamidine, and kept on ice for 30 min. The lysates were cleared by centrifugation, and volume and protein were measured and equalized. Streptavidin beads in 300 μl lysis buffer were added and the mixtures were incubated overnight at 4°C. The beads were washed 5 times with lysis buffer and the bound proteins were released in sample buffer and analysed by Western blot.

Glycosylation assay

HEK cells were transfected with 1 μg of the SLC26A9 vector, and 1 μg of the appropriate WNK vector using 10 μg ml^{-1} of polyethylenimine (Polysciences). After 48 h the cells were lysed in RIPA buffer at 4°C. The lysates were cleared by centrifugation and 100 μl of the supernatants were incubated with 500 units of either Endoglycosidase H (EndoH) or PNGaseF (peptide-*N*-Glycosidase F; NEB) for 1 h at 30°C. The deglycosylation reactions were stopped by the addition of SDS-PAGE sample buffer.

Immunocytochemistry

Control and transfected oocytes were imbedded in OCT reagent, frozen in liquid N_2 and 4 μm sections were cut and immobilized on poly L-lysine-coated cover slips. The sections were permeabilized by incubation with 0.5 ml of cold methanol for 10 min at −20°C. The non-specific sites were blocked with 5% goat serum, 1% BSA, and 0.1% gelatin in PBS (blocking medium) and the sections were incubated with 1 : 250 dilution of anti-STAS-domain antibodies (a gift from Phil Thomas, UT Southwestern Medical Center, Dallas, TX, USA) in blocking medium overnight at 4°C. The anti-STAS-domain antibodies were raised against recombinantly expressed and purified SLC26A3 STAS domain and were found to recognize several SLC26 transporters, including SLC26A9. After washing the bound antibodies were detected with anti-IgG tagged with fluorescein isothiocyanate (FITC). Images were captured with a Bio-Rad MRC 1024 confocal microscope.

Simultaneous measurement of current (or membrane potential), pH_i and Cl^-_i in *Xenopus* oocytes

All procedures for maintaining the frogs and preparation of oocytes followed NIH guidelines and were approved by the Animal Care and Use Committee of UT Southwestern Medical Center. Oocytes were obtained by partial ovariectomy of female *Xenopus laevis* (Xenopus Express, Beverly Hills, FL, USA) that were sedated in a bath consisting of a 0.2% methanesulphonate salt of 3-aminobenzoic acid ethyl ester (Sigma) and placed on ice. The abdomen was opened and a small piece of ovary ($\sim$1 cm^2) was removed. The abdomen was then closed and sutured. The frogs were allowed to slowly recover from anaesthesia by washing with warm water while vital signs were monitored. When the frogs were fully recovered, they were transferred to the animal facility and kept in a separate tank for 24 h after surgery before returning to the home tank. Each frog was used only twice to obtain oocytes, once from each side, with an interval of 2 months before the second removal. Electrophysiological recordings were performed at room temperature with two-electrode voltage clamp or current clamp methods, as previously described (Shcheynikov *et al.* 2006). Briefly, SLC26A9 current was recorded with an OC-725C Oocyte Clamp Amplifier (Warner Instrument Corp.). Current and voltage were digitized at 500 Hz and then filtered at 100 Hz using a Digidata 1322A A/D converter and analysed using the Clampex 8.1 software. The current was measured by stepping the membrane potential from a holding potential of −30 mV to 0 mV, and then the membrane potentials were stepped between −100 and +60 mV at 10 mV steps for 200 ms with a 500 ms interval between steps.

Oocytes were injected with 50 nl water (controls) or 50 nl water containing between 4 and 5 ng of each of the cRNAs of interest and were used 3–5 days post injection. The oocytes were bathed in ND-96 solution or ND-96 solution in which the Cl^- was replaced with other anions as follows. The standard oocytes ND-96 solution contained (mM): 96 NaCl, 2 KCl, 1.8 $CaCl_2$, 1 $MgCl_2$, 2.5 pyruvate, 5 Hepes-Na, pH 7.5 (103.6 Cl^-) or a solution in which 25 mM NaCl was replaced with 25 mM sodium gluconate (78.6 Cl^-). The HCO_3-buffered solution contained (mM): 71 NaCl, 25 $NaHCO_3$, 2 KCl, 1.8 $CaCl_2$, 1 $MgCl_2$, 5 Hepes-Na, pH 7.5 (78.6 Cl^-, 25 HCO_3^-). The Hepes-buffered, Cl^--free media contained 96 sodium gluconate, 2 potassium gluconate, 1.8 calcium cyclamate, 1 $MgSO_4$, 5 Hepes-Na,

pH 7.5. The HCO_3^--buffered, Cl^--free media contained 71 sodium gluconate, 25 $NaHCO_3$, 2 potassium gluconate, 1.8 calcium cyclamate, 1 $MgSO_4$, 5 Hepes-Na, pH 7.5. HCO_3^--buffered solutions were gassed with 5% CO_2–95% O_2. The Cl^--free media were used to prepare media in which the major anion was NO_3^-, Br^- or I^- by replacing the sodium gluconate with the respective Na^+ salt so that the solution contained 96 mM Br^-, I^- or NO_3^-. Current and voltage are digitized via an A/D converter and analysed by Clampex 8.1. For pH_i measurement, the tip of the pH electrode was filled with 0.5 μl of a H^+ exchanger resin and the electrodes were backfilled with ND-96 solution and calibrated in standard solutions of pH 6, 7 and 8. Calibration of the pH electrode was the same in solutions containing 110 or 10 mM Cl^-. The electrodes were fitted with a holder with an Ag–AgCl wire attached to a high-impedance probe of a two-channel electrometer. A second channel was used for the measurement of membrane potential and the bath was grounded via a 3 M KCl agar-bridge connected to an Ag–AgCl wire. The signal from the voltage electrode was subtracted from the voltage of the pH electrode to obtain pH_i. Cl^-_i was measured with a Cl^--sensitive liquid ion exchanger. The tips of the electrodes were filled with the Cl^--selective ion exchanger and backfilled with 3 M KCl. The electrodes were calibrated in solutions containing 1, 3, 10, 30 and 100 mM Cl^-. The calibration was the same at pH 6.5 and 7.5. For simultaneous measurement of pH_i and Cl^-_i, the oocytes were impaled with three electrodes. In this case, two ion-sensitive electrodes were connected to the FD-223 electrometer, and one reference microelectrode was used to record membrane potential with the OC-725C amplifier. HCO_3^- and Cl^- fluxes were determined from the first derivative of the slopes of pH_i and Cl^-_i changes in response to removal of Cl^-_o.

Current measurement in HEK cells

The whole-cell Cl^- current was measured at room temperature in control and HEK cells transfected with SLC26A9 and the WNKs as previously described (Ko *et al.* 2004). The Cl^- current was isolated using a pipette solution containing (mM): 140 *N*-methyl-D-glucamine (NMDG)-Cl, 1 $MgCl_2$, 2 EGTA, 0.5 ATP, and 10 Hepes (pH 7.3 with Tris), and a bath solution composed of (mM): 145 NMDG-Cl, 1 $MgCl_2$, 1 $CaCl_2$, 10 Hepes (pH 7.4 with NaOH), and 10 glucose. Cl^--free solutions were prepared by replacing Cl^- with gluconate and using $MgSO_4$. The current was recorded with an Axopatch 200B patch-clamp amplifier and was filtered at 2 kHz and digitized at 1 kHz. The membrane conductance was probed by stepping the membrane potential from a holding potential of 0 mV to membrane potentials between −100 and +100 mV at 20 mV steps. Pipettes had resistances between 5 and 7 MΩ when filled with an intracellular solution. The seal resistance was higher than 8 GΩ. Current recording and analysis were performed with the Clampex 8.1 software.

Results

SLC26A9 is a Cl^- channel

To study the properties of SLC26A9 we first expressed the protein in *Xenopus* oocytes, in which it is possible to simultaneously measure membrane potential or membrane current, pH_i and Cl^-_i (Shcheynikov *et al.* 2006). Expression of SLC26A9 in the oocytes resulted in a large Cl^- current. Figure 1*A* shows the instantaneous current plots and Fig. 1*B* shows the *I–V* relationships recorded from oocytes incubated in Hepes- or HCO_3^--buffered media and in the presence and absence of extracellular Cl^- (Cl^-_o). The SLC26A9 current does

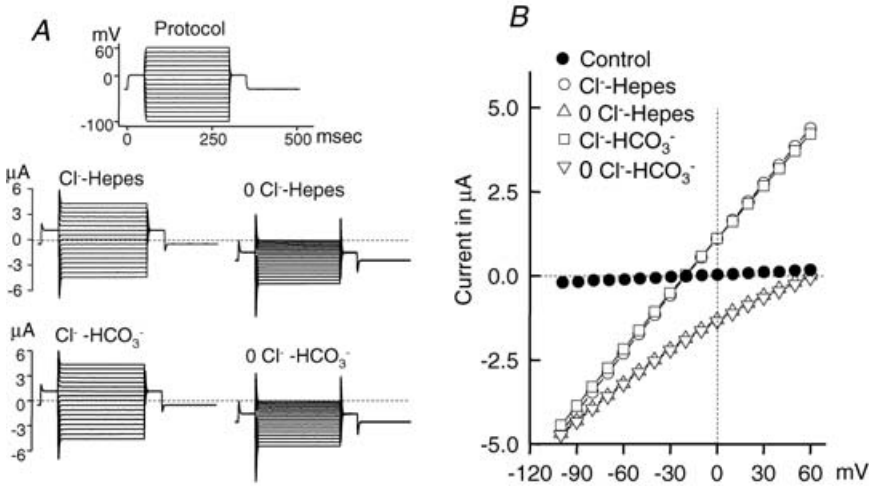

Figure 1. SLC26A9 conducts Cl^-
A, instantaneous current recorded in oocytes bathed in Hepes- or HCO_3^--buffered media and in the presence or absence of Cl^-. *B*, *I–V* relationships of current measured in control oocytes (●) or *Xenopus* oocytes expressing SLC26A9 when incubated in Hepes- (○, △) or HCO_3^--buffered media (□, ▽) in which the major anion is Cl^- (○, □) or gluconate (0 Cl^-, △, ▽). Representative traces are shown. The mean ± S.E.M. of 28 similar experiments is given in the text.

not show any time- or voltage-dependent regulation in the presence or absence of HCO_3^- (Fig. 1*A*). In Hepes-buffered media the current averaged $6.2 \pm 0.5\ \mu A$ (mean ± S.E.M.) at +60 mV with a reversal potential of -23 ± 1 mV ($n = 28$). Cl^-_i in oocytes expressing SLC26A9 was measured to be 27.4 ± 2.7 mM ($n = 14$), which results in a calculated reversal potential of -27 ± 2.6 mV that is in good agreement with the measured reversal potential. Replacing Cl^-_o with gluconate (Glu^-) shifted the reversal potential to $+50.6 \pm 1.5$ mV. Incubating the same oocytes in HCO_3^--buffered media had no measurable effect on the size of the current or the reversal potential in the presence and absence of Cl^-_o (Fig. 1*B*), providing the first evidence that SLC26A9 primarily conducts Cl^- and has minimal HCO_3^- permeability.

To further characterize the SLC26A9-mediated current we measured its selectivity to different anions. Figure 2*A* and the summary in Fig. 2*C* shows that SLC26A9 conducts Br^- slightly better than Cl^-, with replacement of Cl^-_o with Br^-_o increasing the outward current by 1.12 (±0.02)-fold ($n = 9$, $P < 0.05$). On the other hand, both I^- and NO_3^- reduced the current, indicating that SLC26A9 anion conductance followed the rank order $Br^- > Cl^- > I^- > NO_3^- > Glu^-$. Significantly, I^- and NO_3^- reduced both the outward (their own) and inward (Cl^-) currents. This is illustrated in Fig. 2*B* for I^-, which also shows that inhibition of the Cl^- current by I^- is fast, and completely but slowly reverses upon replacing the I^- with Cl^-_o.

Figure 2*A* shows that the anions also affected the reversal potential. This is illustrated in more detail in Fig. 3. Figure 3 also compares the selectivity of SLC26A9 and SLC26A7 for the anions. Figure 3*A* and *B* shows that while replacing Cl^-_o with Glu^- strongly depolarized the cells, replacing Cl^-_o with all other anions hyperpolarized the membrane potential of cells expressing SLC26A9. This suggests that the selectivity of SLC26A9 for the tested anions follows the rank order $I^- > Br^- > NO_3^- > Cl^- > Glu^-$ and the reduced current observed with NO_3^- and I^- (Fig. 2) is due to reduced conductance of the channel for these anions. By contrast, SLC26A7 displays higher selectivity and conductance for NO_3^- over Cl^-. Figure 3*C* and *D* shows that replacing Cl^-_o with NO_3^- hyperpolarized oocytes expressing SLC26A7 and markedly increased the SLC26A7-mediated current.

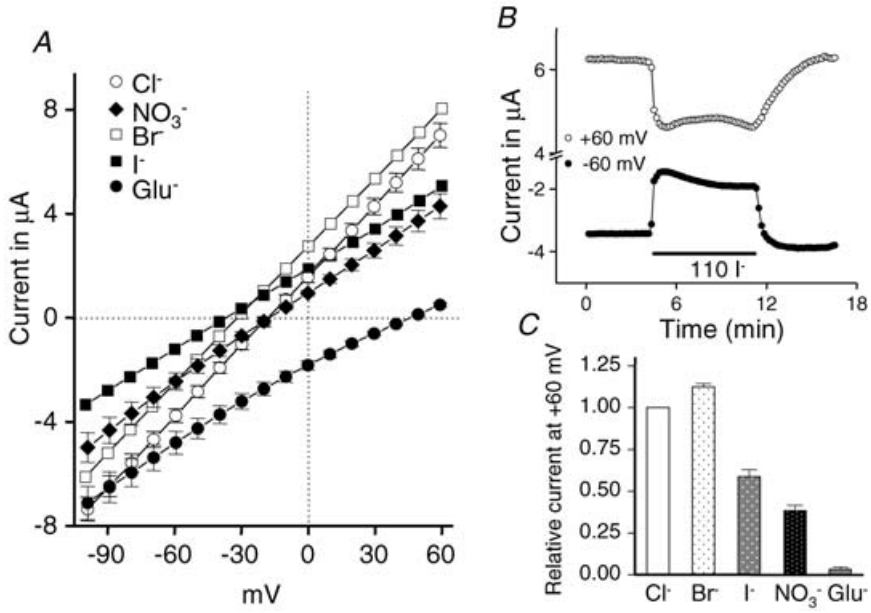

Figure 2. SLC26A9-mediated anion currents
A, current measured in *Xenopus* oocytes expressing SLC26A9 and incubated in Hepes-buffered media containing either 103.6 mM Cl^- (○) or 96 mM of the following anions: NO_3^- (♦), Br^- (□), I^- (■), gluconate (Glu^-, ●). Means from 9–14 oocytes are shown for the current recorded in the presence of Cl^-, Glu^- and NO_3^-, while for clarity single traces are shown for the current recorded with Br^- and I^-. The oocyte was incubated for 10 min in Cl^--containing media after exposure of the oocyte to the ion of interest for 3 min to allow recovery of Cl^-_i between solution changes. *B*, time course of outward and inward current inhibition by I^-. Current was measured by holding the membrane potential at −30 mV and every 5 s stepping to +60 and −60 mV for 200 ms. The oocytes were perfused with ND-96 containing 103.6 mM Cl^- and then with a solution in which Cl^- was replaced with I^-. *C*, current measured at +60 mV with each of the anions relative to the Cl^- current measured in the same oocytes using the protocol in *A*. For all anions the current was statistically different from that measured with Cl^- at $P < 0.05$ or better by one-way ANOVA. The mean ± S.E.M. of 9 similar experiments is given in the text.

Sensitivity to Cl^- transport inhibitors

Useful information for a Cl^- channel is its sensitivity to common Cl^- channel inhibitors that can then be used to probe for the potential physiological role of the channel. Figure 4 shows that the SLC26A9-mediated Cl^- current is not inhibited by 100 μM diphenylamine-2-carboxylic acid (DPC), 100 μM 5-nitro-2′-(3-phenylpropylamino)-benzoate (NPPB) or 250 μM glibenclamide ($n = 3$ for each). SLC26A9 current is only partially inhibited by DIDS, with 0.1 mM DIDS inhibiting the current by $36 \pm 5\%$ with no further inhibition by increasing DIDS to 1 mM. This was not because of instability of the DIDS since DIDS was freshly prepared on the day of each experiment in DMSO and was diluted at least 200-fold into the perfusion media. On the other hand, both flufenamic and niflumic acids almost completely inhibited the SLC26A9-mediated Cl^- current with similar half-maximal inhibition at about 0.4 mM.

SLC26A9 is a poor HCO_3^- transporter

To determine the Cl^- and HCO_3^- transport capacity of SLC26A9 we measured the effect of HCO_3^- on Cl^- current, membrane potential, Cl^-_i and pH_i in the same cells. The current measurements in Fig. 1 show that HCO_3^- had no measurable effect on the current and the reversal potential in cells bathed in Cl^--containing or Cl^--free media. Hence, the HCO_3^-/Cl^- permeability ratio of SLC26A9 is very low and could not be discerned by current measurements.

In a second protocol we measured the effect of HCO_3^- on the changes in the membrane potential, pH_i and Cl^-_i in response to removal of Cl^-_o. Figure 5*A* and *C* shows that HCO_3^- had a minimal effect of the resting membrane potential and on the depolarization caused by removal of Cl^-_o. However, albeit very low, SLC26A9 does have a measurable HCO_3^- permeability, as revealed by the higher rate of HCO_3^- influx into oocytes expressing SLC26A9 than into control oocytes. This can be seen best in the inset in Fig. 5*B* with the expanded pH and time scales. SLC26A9-mediated HCO_3^- efflux occurred at a rate of 0.33 ± 0.04 mM min^{-1} ($n = 5$). However, the rate of Cl^- efflux observed on Cl^-_o removal was not affected by HCO_3^-.

SLC26A9 is regulated by the WNK kinases

The WNK kinases (WNKs) regulate many Na^+, K^+ and Cl^- transporters (Gamba, 2005; Kahle *et al.* 2005; Subramanya *et al.* 2006; Xie *et al.* 2006), including slc26a6 (Kahle *et al.* 2004), which mediate fluid and electrolyte homeostasis. Therefore, it was of interest to determine whether the WNKs regulate SLC26A9. Oocytes were injected with 4 ng of SLC26A9 cRNA alone or together with 5 ng of either WNK1, WNK3

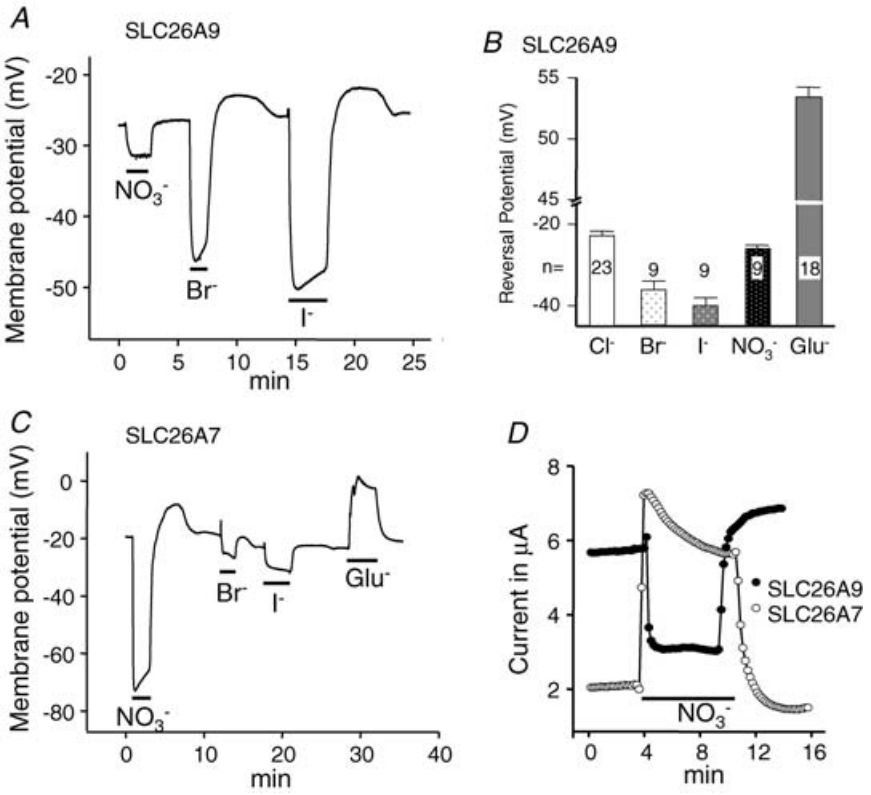

Figure 3. Anionic selectivity of SLC26A9 and SLC26A7
A, representative trace, and *B*, reversal potentials obtained with the indicated anions measured with oocytes expressing SLC26A9. The standard ND-96 solution contained 103.6 mM Cl^- and it was replaced by Cl^--free solution containing 96 mM NO_3^-, Br^- or I^-, as indicated by the bars. Note that the oocytes were incubated with solution ND-96 between solution changes. The numbers in the bars are the number of experiments performed at each condition. *C*, similar measurement in oocytes expressing SLC26A7, illustrating the different anionic selectivity of the two Cl^- channels. Although NO_3^- hyperpolarizes oocytes expressing SLC26A7 and SLC26A9, *D* shows the reduced NO_3^- current by SLC26A9 (●) and increased NO_3^- current by SLC26A7 (○) relative to Cl^-. Current was measured at a holding potential of +60 mV.

or WNK4. Figure 6*A–C* demonstrates that the WNKs inhibit SLC26A9-mediated Cl^- current. In addition, we tested the effect of kinase-deficient WNK3 and WNK4 mutants as well as of the WNK3 kinase domain to determine if the kinase activity of the WNKs is required for the regulation of SLC26A9. The kinase-dead WNK3(K159M) and WNK4(K183) inhibited SLC26A9 to an extent similar to the wild-type WNKs. Moreover, the kinase domain of WNK3, WNK3(1–410), has no effect on SLC26A9 activity. To monitor the cell surface expression of SLC26A9, immunolocalization experiments were performed in oocytes in the presence and absence of the WNKs. Figure 6*D* shows that WNK1, WNK3 and WNK4 all reduce the cell surface expression of SLC26A9.

To extend the findings of Fig. 6 to mammalian cells, we measured the SLC26A9-mediated Cl^- current in HEK 293 cells. Figure 7*A* shows that SLC26A9 expressed in HEK 293 cells generated a large Cl^- current. Figure 7*B* shows that the properties of the instantaneous current were the same as those found in *Xenopus* oocytes (Fig. 1). Moreover, Fig. 7*A* and *C* shows that WNK1 and WNK4 inhibited SLC26A9 current in HEK 293 cells.

Expression of SLC26A9 N-terminally tagged with HA (HA-SLC26A9) in HEK cells invariably ($n = 11$) resulted in two protein products with the lower band corresponding to the SLC26A9 predicted molecular weight of 87 kDa (Fig. 7*D*). To determine the glycosylation state of the two products we treated HEK 293 lysates containing SLC26A9 with EndoH or PNGaseF. Surprisingly, EndoH had no effect on the mobility of either of the two bands. Notably, treatment with PNGaseF increased the mobility of both bands, suggesting that both bands represent mature forms of SLC26A9. We considered the possibility that the two bands were the result of a proteolytic cleavage event. To test this possibility, the expression pattern of HA-SLC26A9-myc, which is tagged at both termini, was analysed. Figure 7*E* shows the same expression and glycosylation pattern when the blot is probed with anti-HA or with anti-myc, indicating that both bands represent full length proteins.

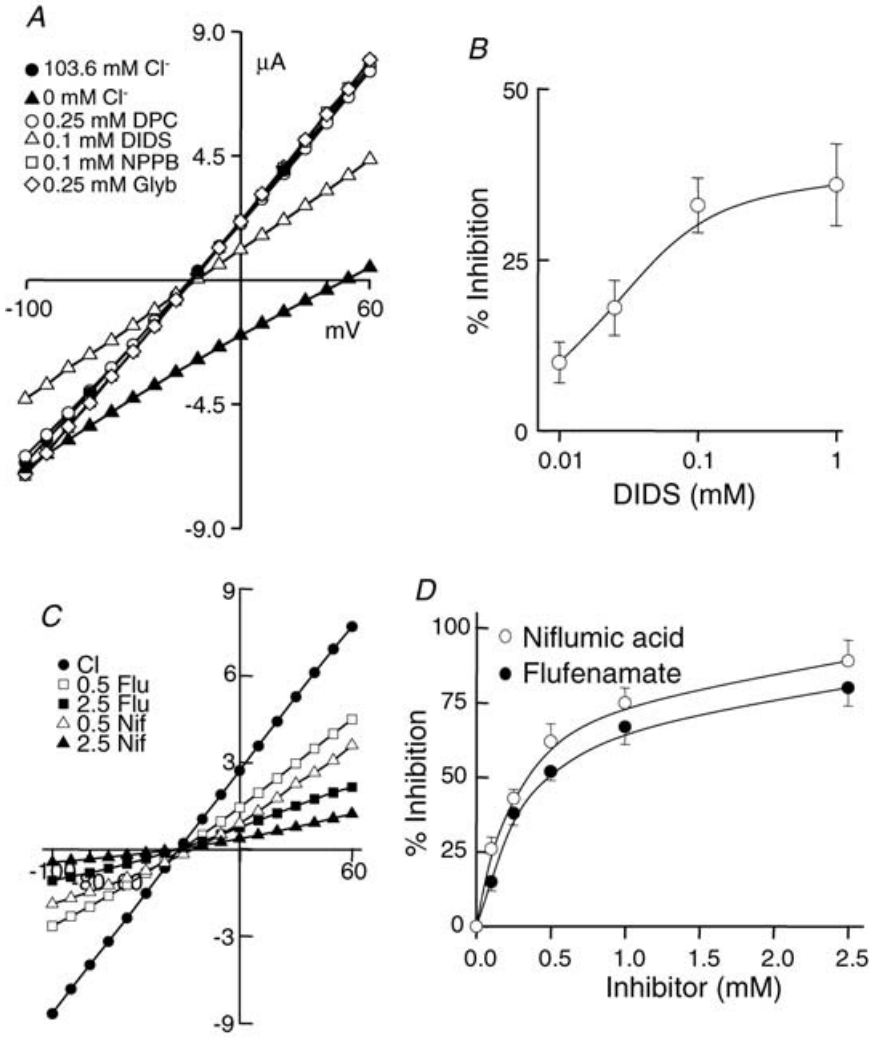

Figure 4. Inhibitor sensitivity of Cl^- current by SLC26A9
A, representative *I–V* relations of Cl^- current in oocytes expressing SLC26A9 in the absence (●) and presence of 250 μM DPC (○), 0.1 mM DIDS (△), 100 μM NPPB (□) or 250 μM glibenclamide (◇). *B*, effect of 0.01–1 mM DIDS on SLC26A9 current. *C*, representative *I–V* relations of Cl^- current in oocytes expressing SLC26A9 in the absence (●) and presence of 0.5 (□) or 2.5 mM (■) flufenamic acid (Flu) or of 0.5 (△) or 2.5 mM (▲) niflumic acid (Nif); *D*, dose–response to niflumic and flufenamic acids. The results in *B* and *D* are the mean ± S.E.M. of 4 experiments.

Figure 7*D–F* shows that coexpression of SLC26A9 with WNK1 and WNK4 had no effect on total expression or the maturation of SLC26A9. This suggests that inhibition of SLC26A9 activity by the WNKs is not due to reduced maturation of SLC26A9, but rather the WNKs affect SLC26A9 after trafficking out of the Golgi. We analysed the effect of the WNKs on surface expression of SLC26A9 by performing biotinylation assays. Figure 7*F* shows the results of a biotinylation assay representative of three (WNK1) and four (WNK4) other experiments. In all experiments the faster 87 kDa migrating SLC26A9 form is the predominant one biotinylated, suggesting that it is the species found in the plasma membrane and functioning as a Cl^- channel. WNK1 and WNK4 markedly reduced surface expression of SLC26A9.

Discussion

In the present work we found that SLC26A9 is a Cl^- channel regulated by the WNK kinases. Previous work used pH_i measurements with the pH-sensitive fluorescent dye BCECF to conclude that SLC26A9 is a DIDS-sensitive Cl^-–HCO_3^- exchanger (J. Xu *et al.* 2005). The only evidence for Cl^-–HCO_3^- exchange activity was an increase in pH_i in response to removal of Cl^-_o. However, the mode of transport responsible for this activity was not determined. In the present work, we measured membrane potential, current, pH_i and Cl^-_i in *Xenopus* oocytes and current in HEK cells. Expression of SLC26A9 in the two cell types resulted in a large Cl^- current. Importantly, HCO_3^- had no effect on the reversal potential or the Cl^- current mediated by SLC26A9. Moreover, HCO_3^- had no effect on the SLC26A9-mediated Cl^- influx or efflux. In comparison, slc26a3 and slc26a6 mediate large HCO_3^- fluxes, HCO_3^- shifted the reversal potential according to the stoichiometry of the exchange and HCO_3^- markedly increased the Cl^- fluxes (Shcheynikov *et al.* 2006). These findings lead us to conclude that SLC26A9 does not function as a Cl^-–HCO_3^- exchanger or significantly contribute to epithelial HCO_3^- secretion. Rather, SLC26A9 functions as a Cl^- channel at the luminal membrane of airway secretory glands and gastric surface

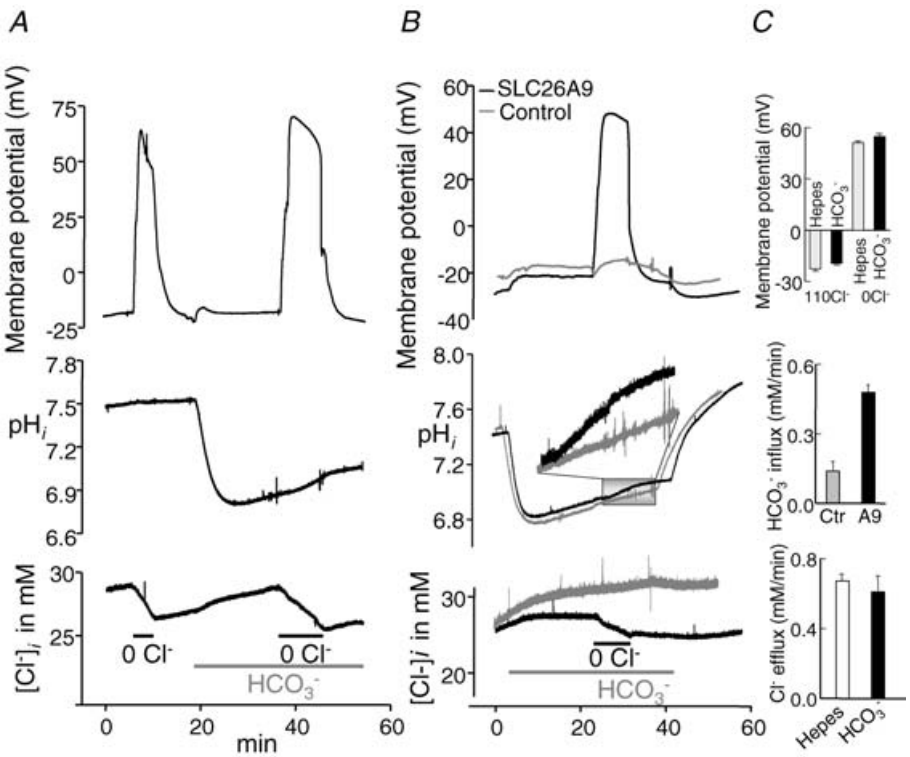

Figure 5. Cl^- and HCO_3^- fluxes by SLC26A9
In *A* and *B* the membrane potential, pH_i and Cl^-_i were measured simultaneously. In *A*, oocytes expressing SLC26A9 were incubated in Hepes-buffered ND-96 media containing 103.6 mM Cl^- and perfused with Hepes-buffered Cl^--free media containing Glu^- (first 0 Cl^-, black bar), with HCO_3^--buffered media containing 25 mM HCO_3^- and 78 mM Cl^- (grey bar) and with HCO_3^--buffered Cl^--free media in which Glu^- replaced Cl^- (second 0 Cl^-, black bar). Note that HCO_3^- had no measurable effect on Cl^- efflux. In *B*, control oocytes (grey traces) and oocytes expressing SLC26A9 (black traces) bathed in HCO_3^--buffered media were exposed to Cl^--free medium for the indicated period. The inset in the pH_i panel shows the changes in pH_i in expanded time and pH scales. The columns in *C* show the mean ± S.E.M. of 4–7 experiments for the indicated conditions.

epithelial cells. This conclusion also means that SLC26A9 does not mediate HCO_3^- secretion by surface gastric epithelial cells as suggested before (J. Xu *et al.* 2005), but more likely controls the Cl^- permeability of the luminal membrane of these cells. This conclusion is further supported by the profile of the blockers' sensitivity to SLC26A9 (Fig. 4). We note that HCO_3^- secretion by gastric surface epithelial cells is electroneutral and is nearly abolished by 0.5 mM DIDS (Allen & Flemstrom, 2005), whereas 0.5 mM DIDS inhibited SLC26A9 activity by only 36%.

Measurement of anion current revealed a difference in the selectivity ($I^- > Br^- > NO_3^- > Cl^- > Glu^-$) and permeability ($Br^- > Cl^- > I^- > NO_3^- > Glu^-$) sequence of SLC26A9 to anions, with NO_3^- and I^- inhibiting the Cl^- conductance. The anomaly of a higher selectivity for NO_3^- but lower conductance is specific for SLC26A9. Slc26a3 (Shcheynikov *et al.* 2006) and SLC26A7 (Fig. 3 and Kim *et al.* 2005) display higher selectivity and conductance for NO_3^- over Cl^-. Figure 3 shows that replacing Cl^-_o with NO_3^- hyperpolarized the oocytes and markedly increased the SLC26A7-mediated current. This is in contrast to the observation with oocytes expressing SLC26A9, in which replacing Cl^- with NO_3^- resulted in lower outward current (NO_3^- influx), although it hyperpolarized the oocytes. We interpret these findings to indicate that NO_3^- can partially block SLC26A9 conductance. That is, the differential selectivity and conductance of I^- and NO_3^- by SLC26A9 may suggest that the channel pore accommodates these anions better than Cl^- and the anions linger within the pore longer than Cl^-. This interpretation is supported by the finding that both I^- and NO_3^- inhibit the Cl^- current and recovery of the Cl^- outward current from an I^- block is slow (Fig. 2).

SLC26A9 activity is prominently regulated by the WNK kinases (WNKs). The WNKs regulate many Na^+, K^+

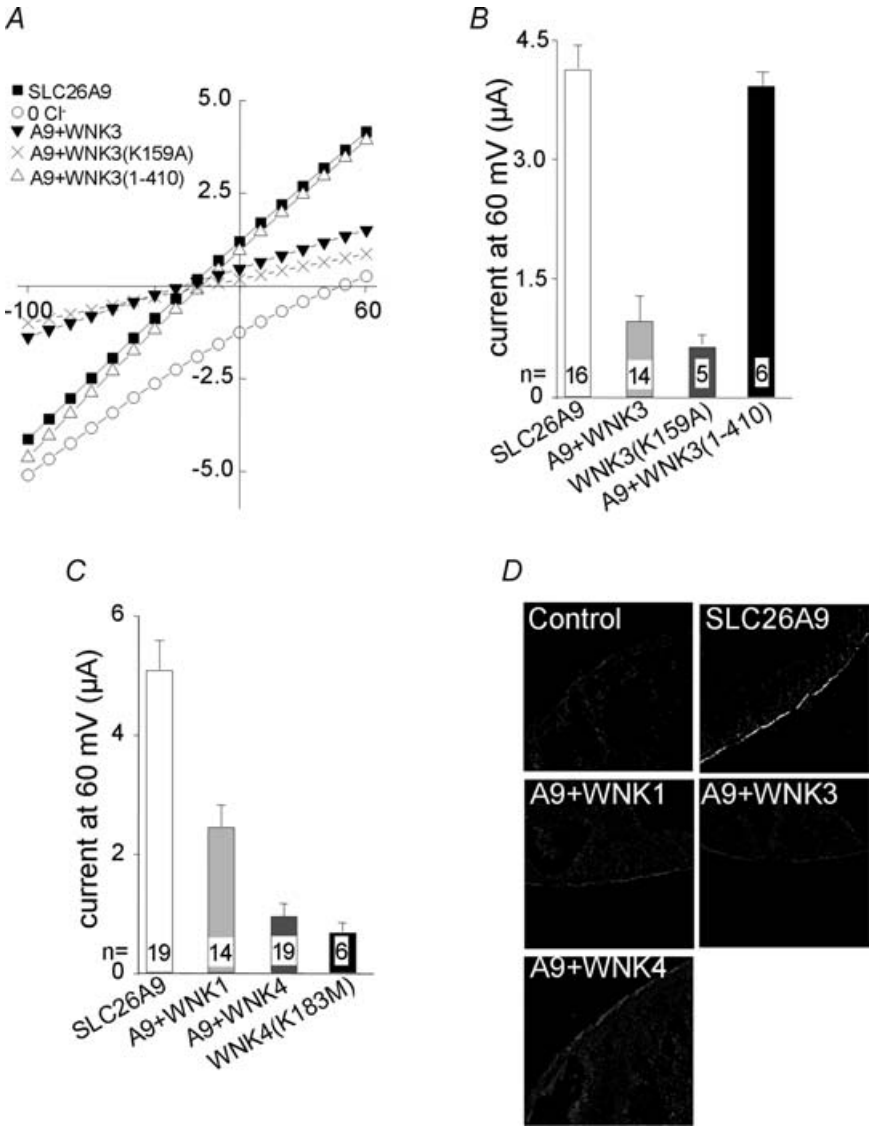

Figure 6. Inhibition of SLC26A9 activity by WNK1, WNK3 and WNK4 expressed in *Xenopus* oocytes
A, *I–V* relationship of oocytes expressing SLC26A9 alone or SLC26A9 and WNK3, SLC26A9 and the kinase-dead WNK3(K159M) or SLC26A9 and the kinase domain of WNK3 (WNK3(1–410)). *B*, summary of results of the indicated number of experiments similar to those in *A*. In *C*, oocytes expressing SLC26A9 alone, SLC26A9 and WNK1, SLC26A9 and WNK4 or SLC26A9 and the kinase-dead mutant of WNK4 (WNK4(K183M)) were used to measure the SLC26A9 Cl^- current. In *D*, slices were cut from a row of 3–4 control oocytes or oocytes expressing SLC26A9 and the indicated WNKs and imbedded in O.C.T. compound. The slices were stained with anti-STAS-domain antibodies prepared against purified STAS domain.

and Cl^- transporters involved in fluid and electrolyte homeostasis (Gamba, 2005; Kahle *et al.* 2005; Subramanya *et al.* 2006; Xie *et al.* 2006), including slc26a6 (Kahle *et al.* 2004). The WNKs can regulate ion transporters directly by phosphorylating the transporters (for example, regulation of NKCC2 and KCC by WNK3; Rinehart *et al.* 2005), by phosphorylating and activating other kinases (for example, activation of ORS1 by WNK1; Anselmo *et al.* 2006), or by acting as a platforms or scaffolds for other proteins which may be involved in endocytosis (Yang *et al.* 2005). In the latter case, the platform function of the WNKs is independent of their kinase activity and is mediated by the C-terminal non-kinase domain of the WNKs (Gamba, 2005; Kahle *et al.* 2005; Subramanya *et al.* 2006; Xie *et al.* 2006). The present work showed that WNK1, WNK3 and WNK4 regulate SLC26A9 activity and that the regulation does not require the kinase activity of the WNKs. These findings suggest that the WNKs act as scaffolds that recruit other proteins that regulate the activity of SLC26A9, similar to the role of WNK4 in the regulation of NCC (Yang *et al.* 2005) and the role of WNK1 in the regulation of the ROMK K^+ channel (Lazrak *et al.* 2006; He *et al.* 2007).

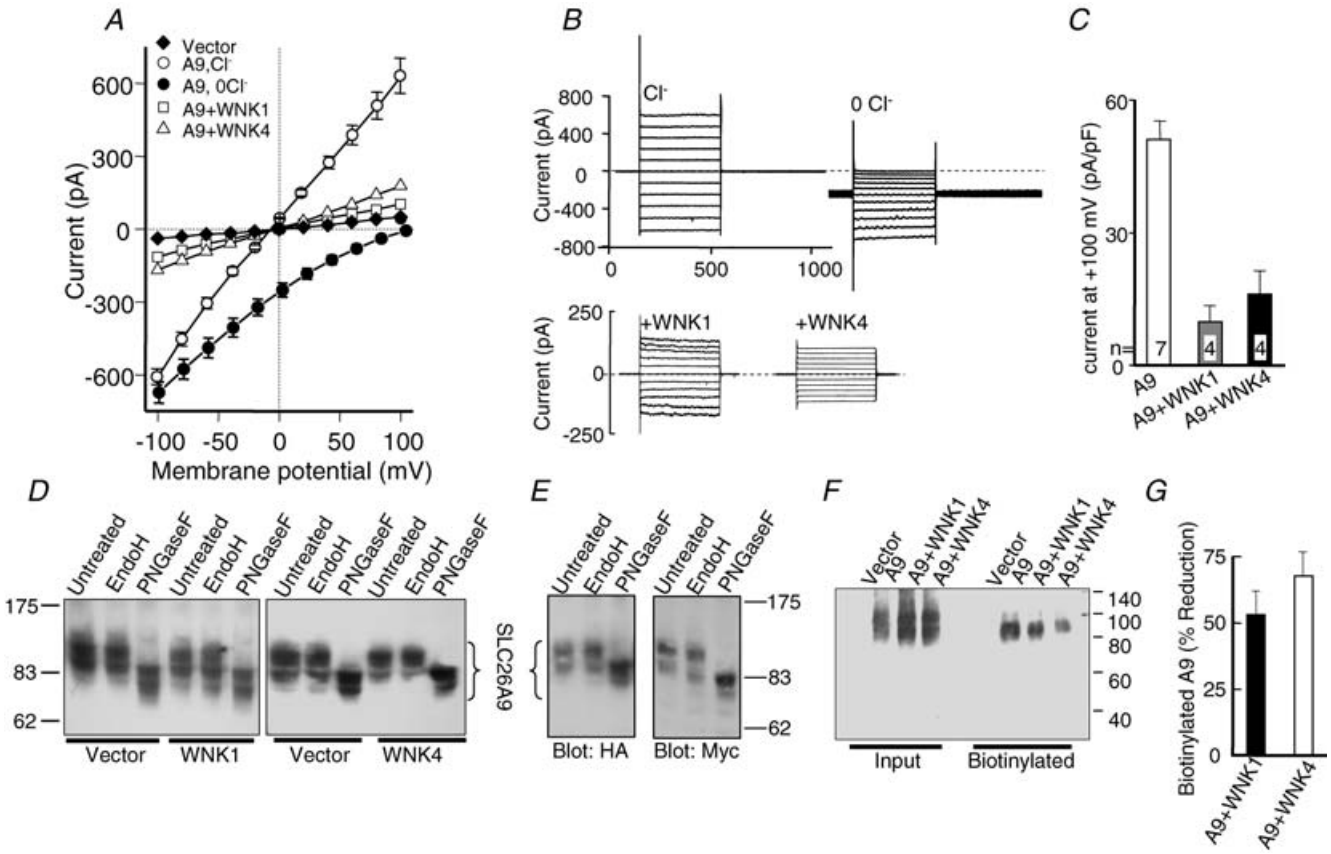

Figure 7. The WNK kinases inhibit current and surface expression of SLC26A9 in HEK cells
A, whole-cell current was measured in HEK cells with pipette and bath solutions containing 150 mM Cl^- (○) or bath solution containing 150 mM Glu^- (●). The cells were transfected with empty vector (♦), SLC26A9 alone (○, ●), SLC26A9 and WNK1 (□) or SLC26A9 and WNK4 (△). Representative *I–V* relationships are shown in this panel. For clarity, the *I–V* relationships with the WNKs are from single experiments with the means summarized in *C*. *B* shows the instantaneous SLC26A9 current in the presence of 150 mM bath Cl^- or 150 mM Glu^- for cells expressing SLC26A9 (top traces) or SLC26A9 + WNK1, and SLC26A9 + WNK4 (bottom traces). *C*, summary of the results from the indicated number of experiments obtained with HEK cells expressing SLC26A9 alone (open column), SLC26A9 and WNK1 (grey column), or SLC26A9 and WNK4 (black column). In *D*, HEK cells expressing SLC26A9 and empty vector, SLC26A9 and WNK1, or SLC26A9 and WNK4, were used to prepare extracts. The extracts were treated with EndoH or PNGaseF to analyse the glycosylation state of SLC26A9. In *E*, doubly tagged HA-SLC26A9-myc was expressed in HEK cells to analyse the expression and glycosylation pattern by probing the blots for the N- (anti-HA) or C-termini (anti-myc) of SLC26A9. In *F*, HEK cells transfected with empty vector, HA-SLC26A9, HA-SLC26A9 + WNK1, or HA-SLC26A9 + WNK4, were used to analyse the effects of the WNKs on total (input) and surface expression (biotinylated) of SLC26A9. *G*, summary of the percentage reduction in surface expression of SLC26A9 by the WNKs. The results are the mean ± S.E.M. of 3 (WNK1) and 4 (WNK4) experiments.

Regulation by the WNKs has been shown to invariably involve surface expression of the transporters (Gamba, 2005; Kahle *et al.* 2005; Subramanya *et al.* 2006; Xie *et al.* 2006; He *et al.* 2007). The vast majority of the studies describing the effects of the WNKs on the activity and surface expression of the transporters have been performed in *Xenopus* oocytes (Gamba, 2005; Kahle *et al.* 2005; Subramanya *et al.* 2006; Xie *et al.* 2006). In fact, only one study has shown an effect of a WNK in mammalian cells, a study that showed WNK4 regulated the surface expression of the NaCl cotransporter NCCT (Cai *et al.* 2006). It is important to demonstrate that the observed effect of the WNKs in oocytes is similar to the effect of the WNKs in mammalian cells. Moreover, protein trafficking and surface expression are markedly affected by temperature, and oocytes are maintained at 18°C. Therefore, we sought to determine if SLC26A9 functions as a Cl^- channel when expressed in mammalian cells. Our results indicated that SLC26A9 is a Cl^- channel in mammalian cells, and analysis of surface expression in HEK cells showed that WNK1 and WNK4 reduced the surface expression of the transporter.

Another surprising finding in the present work is that SLC26A9 is expressed as two mature protein products with the lower 87 kDa band corresponding to the predicted molecular weight. Only the 87 kDa band was targeted to the plasma membrane. N- and C-terminal tagging and glycosylation analysis excluded the possibility that the 87 kDa protein product arises from a proteolytic cleavage of the longer 115 kDa SLC26A9 form. Expression of SLC26A9 as two protein products with only one of them trafficking to the cell surface raises the possibility that the 115 kDa form represents a post translational modification of SLC26A9 that causes it to be retained intracellularly. Processing of the 115 kDa form may be required for its insertion into the plasma membrane where it can then function as a Cl^- channel. Alternatively, since generation of the two forms does not appear to involve cleavage, and both represent mature forms of the protein, it is equally possible that the two forms are stable SLC26A9 species that are targeted to different cellular compartments depending on their processing. Further work is needed to examine these possibilities.

The physiological function of SLC26A9 is not obvious from its tissue distribution or functional properties, in particular in the airway where CFTR is the dominant Cl^- channel at the luminal membrane that regulates the overall secretory process (Ballard & Inglis, 2004). However, the same uncertainty exists with respect to other luminal Cl^- channels, such as the Ca^{2+}-activated Cl^- channel and the outward rectifying Cl^- channel. Nevertheless, a unique feature of the SLC26 transporters is that they are regulated by CFTR and they also regulate CFTR activity (Ko *et al.* 2002, 2004). The mutual regulation is mediated by the CFTR R domain and the SLC26 transporters STAS domain (Ko *et al.* 2004). Since SLC26A9 is expressed in the luminal membrane of airway secretory cells (Lohi *et al.* 2002), it is possible that SLC26A9 regulates CFTR activity in the luminal membrane. Moreover, SLC26A9 can function as CFTR-regulated Cl^- channel which could mediate a substantial portion of the Cl^- conductance of the luminal membrane in the stimulated cells. Indeed, the author's preliminary unpublished observations in which SLC26A9 activity was measured as Cl^--dependent OH^- fluxes indicate that SLC26A9 is activated by CFTR (data not shown).

Regulation by the WNKs may have a general function in epithelia. The present work shows regulation of SLC26A9 by the WNKs. A recent study reported regulation of CFTR activity by WNK1 and WNK4 (Yang *et al.* 2007). The WNKs reduce the activity of both channels. It is possible that the WNKs are active in the resting state to prevent unnecessary fluid secretion. Another possibility is that the WNKs may mediate the action of inhibitory agonists such as substance P (Ashton *et al.* 1990) and AVP (Ko *et al.* 1999) acting on the pancreatic duct. Although only minimal evidence exists, the activity of the WNKs is regulated by receptor-mediated cell stimulation (reviewed in Subramanya *et al.* 2006; Xie *et al.* 2006).

Another possible role for the regulation of SLC26A9 by the WNKs is that it may mediate the response of the airway and surface gastric epithelial cells to stress and insult. Thus, WNK1, and perhaps other WNKs, exists in complex with the oxidative stress-responsive kinase and both kinases are required for regulation of NKCC1 (Anselmo *et al.* 2006). Indeed, regulation of SLC26A9 by the WNKs is independent of their kinase activity. This indicates that the WNKs function as scaffolds to recruit other proteins, perhaps other kinases, which regulate surface expression of SLC26A9. Such regulation is observed in response to cellular stress, including cell swelling and cell shrinkage. These findings suggest that the WNKs are sensors of cell stress and tonicity. Therefore, the WNKs may transmit the response of the airway and gastric gland to stress or insult by activation of SLC26A9.

References

Allen A & Flemstrom G (2005). Gastroduodenal mucus bicarbonate barrier: protection against acid and pepsin. *Am J Physiol Cell Physiol* **288**, C1–C19.

Anselmo AN, Earnest S, Chen W, Juang YC, Kim SC, Zhao Y & Cobb MH (2006). WNK1 and OSR1 regulate the Na^+, K^+, $2Cl^-$ cotransporter in HeLa cells. *Proc Natl Acad Sci U S A* **103**, 10883–10888.

Ashton N, Argent BE & Green R (1990). Effect of vasoactive intestinal peptide, bombesin and substance P on fluid secretion by isolated rat pancreatic ducts. *J Physiol* **427**, 471–482.

Ballard ST & Inglis SK (2004). Liquid secretion properties of airway submucosal glands. *J Physiol* **556**, 1–10.

Binder HJ, Rajendran V, Sadasivan V & Geibel JP (2005). Bicarbonate secretion: a neglected aspect of colonic ion transport. *J Clin Gastroenterol* **39**, S53–S58.

Cai H, Cebotaru V, Wang YH, Zhang XM, Cebotaru L, Guggino SE & Guggino WB (2006). WNK4 kinase regulates surface expression of the human sodium chloride cotransporter in mammalian cells. *Kidney Int* **69**, 2162–2170.

Chan HC, Shi QX, Zhou CX, Wang XF, Xu WM, Chen WY, Chen AJ, Ni Y & Yuan YY (2006). Critical role of CFTR in uterine bicarbonate secretion and the fertilizing capacity of sperm. *Mol Cell Endocrinol* **250**, 106–113.

Curci S, Debellis L, Caroppo R & Fromter E (1994). Model of bicarbonate secretion by resting frog stomach fundus mucosa. I. Transepithelial measurements. *Pflugers Arch* **428**, 648–654.

de Los Heros P, Kahle KT, Rinehart J, Bobadilla NA, Vazquez N, San Cristobal P, Mount DB, Lifton RP, Hebert SC & Gamba G (2006). WNK3 bypasses the tonicity requirement for K-Cl cotransporter activation via a phosphatase-dependent pathway. *Proc Natl Acad Sci U S A* **103**, 1976–1981.

Dossena S, Rodighiero S, Vezzoli V, Bazzini C, Sironi C, Meyer G, Furst J, Ritter M, Garavaglia ML, Fugazzola L, Persani L, Zorowka P, Storelli C, Beck-Peccoz P, Botta G & Paulmichl M (2006). Fast fluorometric method for measuring pendrin (SLC26A4) Cl-/I- transport activity. *Cell Physiol Biochem* **18**, 67–74.

Everett LA, Glaser B, Beck JC, Idol JR, Buchs A, Heyman M, Adawi F, Hazani E, Nassir E, Baxevanis AD, Sheffield VC & Green ED (1997). Pendred syndrome is caused by mutations in a putative sulphate transporter gene (PDS). *Nat Genet* **17**, 411–422.

Gamba G (2005). Molecular physiology and pathophysiology of electroneutral cation-chloride cotransporters. *Physiol Rev* **85**, 423–493.

He G, Wang HR, Huang SK & Huang CL (2007). Intersectin links WNK kinases to endocytosis of ROMK1. *J Clin Invest* **117**, 1078–1087.

Henriksnas J, Phillipson M, Storm M, Engstrand L, Soleimani M & Holm L (2006). Impaired mucus–bicarbonate barrier in *Helicobacter pylori*-infected mice. *Am J Physiol Gastrointest Liver Physiol* **291**, G396–G403.

Kahle KT, Gimenez I, Hassan H, Wilson FH, Wong RD, Forbush B, Aronson PS & Lifton RP (2004). WNK4 regulates apical and basolateral Cl^- flux in extrarenal epithelia. *Proc Natl Acad Sci U S A* **101**, 2064–2069.

Kahle KT, Wilson FH & Lifton RP (2005). Regulation of diverse ion transport pathways by WNK4 kinase: a novel molecular switch. *Trends Endocrinol Metab* **16**, 98–103.

Kim KH, Shcheynikov N, Wang Y & Muallem S (2005). SLC26A7 is a Cl^- channel regulated by intracellular pH. *J Biol Chem* **280**, 6463–6470.

Kim JY, Zeng W, Kiselyov K, Yuan JP, Dehoff MH, Mikoshiba K, Worley PF & Muallem S (2006). Homer 1 mediates store- and inositol 1,4,5-trisphosphate receptor-dependent translocation and retrieval of TRPC3 to the plasma membrane. *J Biol Chem* **281**, 32540–32549.

Ko SB, Naruse S, Kitagawa M, Ishiguro H, Murakami M & Hayakawa T (1999). Arginine vasopressin inhibits fluid secretion in guinea pig pancreatic duct cells. *Am J Physiol Gastrointest Liver Physiol* **277**, G48–G54.

Ko SB, Shcheynikov N, Choi JY, Luo X, Ishibashi K, Thomas PJ, Kim JY, Kim KH, Lee MG, Naruse S & Muallem S (2002). A molecular mechanism for aberrant CFTR-dependent HCO_3^- transport in cystic fibrosis. *EMBO J* **21**, 5662–5672.

Ko SB, Zeng W, Dorwart MR, Luo X, Kim KH, Millen L, Goto H, Naruse S, Soyombo A, Thomas PJ & Muallem S (2004). Gating of CFTR by the STAS domain of SLC26 transporters. *Nat Cell Biol* **6**, 343–350.

Lazrak A, Liu Z & Huang CL (2006). Antagonistic regulation of ROMK by long and kidney-specific WNK1 isoforms. *Proc Natl Acad Sci U S A* **103**, 1615–1620.

Leng Q, Kahle KT, Rinehart J, MacGregor GG, Wilson FH, Canessa CM, Lifton RP & Hebert SC (2006). WNK3, a kinase related to genes mutated in hereditary hypertension with hyperkalaemia, regulates the K^+ channel ROMK1 (Kir1.1). *J Physiol* **571**, 275–286.

Linsdell P, Tabcharani JA, Rommens JM, Hou YX, Chang XB, Tsui LC, Riordan JR & Hanrahan JW (1997). Permeability of wild-type and mutant cystic fibrosis transmembrane conductance regulator chloride channels to polyatomic anions. *J Gen Physiol* **110**, 355–364.

Liu XZ, Ouyang XM, Xia XJ, Zheng J, Pandya A, Li F, Du LL, Welch KO, Petit C, Smith RJ, Webb BT, Yan D, Arnos KS, Corey D, Dallos P, Nance WE & Chen ZY (2003). Prestin, a cochlear motor protein, is defective in non-syndromic hearing loss. *Hum Mol Genet* **12**, 1155–1162.

Lohi H, Kujala M, Makela S, Lehtonen E, Kestila M, Saarialho-Kere U, Markovich D & Kere J (2002). Functional characterization of three novel tissue-specific anion exchangers SLC26A7 -A8, and -A9. *J Biol Chem* **277**, 14246–14254.

Makela S, Kere J, Holmberg C & Hoglund P (2002). SLC26A3 mutations in congenital chloride diarrhea. *Hum Mutat* **20**, 425–438.

Melvin JE, Yule D, Shuttleworth T & Begenisich T (2005). Regulation of fluid and electrolyte secretion in salivary gland acinar cells. *Annu Rev Physiol* **67**, 445–469.

Min X, Lee BH, Cobb MH & Goldsmith EJ (2004). Crystal structure of the kinase domain of WNK1, a kinase that causes a hereditary form of hypertension. *Structure* **12**, 1303–1311.

Mount DB & Romero MF (2004). The SLC26 gene family of multifunctional anion exchangers. *Pflugers Arch* **447**, 710–721.

Naray-Fejes-Toth A, Snyder PM & Fejes-Toth G (2004). The kidney-specific WNK1 isoform is induced by aldosterone and stimulates epithelial sodium channel-mediated Na^+ transport. *Proc Natl Acad Sci U S A* **101**, 17434–17439.

Poulsen JH, Fischer H, Illek B & Machen TE (1994). Bicarbonate conductance and pH regulatory capability of cystic fibrosis transmembrane conductance regulator. *Proc Natl Acad Sci U S A* **91**, 5340–5344.

Rinehart J, Kahle KT, de Los Heros P, Vazquez N, Meade P, Wilson FH, Hebert SC, Gimenez I, Gamba G & Lifton RP (2005). WNK3 kinase is a positive regulator of NKCC2 and NCC, renal cation-Cl^- cotransporters required for normal blood pressure homeostasis. *Proc Natl Acad Sci U S A* **102**, 16777–16782.

Shcheynikov N, Kim KH, Kim KM, Dorwart MR, Ko SB, Goto H, Naruse S, Thomas PJ & Muallem S (2004). Dynamic control of cystic fibrosis transmembrane conductance regulator Cl^-/HCO_3^- selectivity by external Cl^-. *J Biol Chem* **279**, 21857–21865.

Shcheynikov N, Wang Y, Park M, Ko SB, Dorwart M, Naruse S, Thomas PJ & Muallem S (2006). Coupling modes and stoichiometry of Cl^-/HCO_3^- exchange by slc26a3 and slc26a6. *J Gen Physiol* **127**, 511–524.

Steward MC, Ishiguro H & Case RM (2005). Mechanisms of bicarbonate secretion in the pancreatic duct. *Annu Rev Physiol* **67**, 377–409.

Subramanya AR, Yang CL, McCormick JA & Ellison DH (2006). WNK kinases regulate sodium chloride and potassium transport by the aldosterone-sensitive distal nephron. *Kidney Int* **70**, 630–634.

Superti-Furga A, Hastbacka J, Wilcox WR, Cohn DH, van der Harten HJ, Rossi A, Blau N, Rimoin DL, Steinmann B, Lander ES & Gitzelmann R (1996). Achondrogenesis type IB is caused by mutations in the diastrophic dysplasia sulphate transporter gene. *Nat Genet* **12**, 100–102.

Wall SM (2005). Recent advances in our understanding of intercalated cells. *Curr Opin Nephrol Hypertens* **14**, 480–484.

Wang XF, Zhou CX, Shi QX, Yuan YY, Yu MK, Ajonuma LC, Ho LS, Lo PS, Tsang LL, Liu Y, Lam SY, Chan LN, Zhao WC, Chung YW & Chan HC (2003). Involvement of CFTR in uterine bicarbonate secretion and the fertilizing capacity of sperm. *Nat Cell Biol* **5**, 902–906.

Wilson FH, Disse-Nicodeme S, Choate KA, Ishikawa K, Nelson-Williams C, Desitter I, Gunel M, Milford DV, Lipkin GW, Achard JM, Feely MP, Dussol B, Berland Y, Unwin RJ, Mayan H, Simon DB, Farfel Z, Jeunemaitre X & Lifton RP (2001). Human hypertension caused by mutations in WNK kinases. *Science* **293**, 1107–1112.

Wine JJ (2006). Acid in the airways. Focus on 'Hyperacidity of secreted fluid from submucosal glands in early cystic fibrosis'. *Am J Physiol Cell Physiol* **290**, C669–C671.

Wright AM, Gong X, Verdon B, Linsdell P, Mehta A, Riordan JR, Argent BE & Gray MA (2004). Novel regulation of cystic fibrosis transmembrane conductance regulator (CFTR) channel gating by external chloride. *J Biol Chem* **279**, 41658–41663.

Xie J, Craig L, Cobb MH & Huang CL (2006). Role of with-no-lysine [K] kinases in the pathogenesis of Gordon's syndrome. *Pediatr Nephrol* **21**, 1231–1236.

Xie Q, Welch R, Mercado A, Romero MF & Mount DB (2002). Molecular characterization of the murine Slc26a6 anion exchanger: functional comparison with Slc26a1. *Am J Physiol Renal Physiol* **283**, F826–F838.

Xu B, English JM, Wilsbacher JL, Stippec S, Goldsmith EJ & Cobb MH (2000). WNK1, a novel mammalian serine/threonine protein kinase lacking the catalytic lysine in subdomain II. *J Biol Chem* **275**, 16795–16801.

Xu J, Henriksnas J, Barone S, Witte D, Shull GE, Forte JG, Holm L & Soleimani M (2005). SLC26A9 is expressed in gastric surface epithelial cells, mediates Cl^-/HCO_3^- exchange, and is inhibited by NH_4^+. *Am J Physiol Cell Physiol* **289**, C493–C505.

Xu BE, Min X, Stippec S, Lee BH, Goldsmith EJ & Cobb MH (2002). Regulation of WNK1 by an autoinhibitory domain and autophosphorylation. *J Biol Chem* **277**, 48456–48462.

Xu BE, Stippec S, Chu PY, Lazrak A, Li XJ, Lee BH, English JM, Ortega B, Huang CL & Cobb MH (2005). WNK1 activates SGK1 to regulate the epithelial sodium channel. *Proc Natl Acad Sci U S A* **102**, 10315–10320.

Yang CL, Liu X, Paliege A, Zhu X, Bachmann S, Dawson DC & Ellison DH (2007). WNK1 and WNK4 modulate CFTR activity. *Biochem Biophys Res Commun* **353**, 535–540.

Yang CL, Zhu X, Wang Z, Subramanya AR & Ellison DH (2005). Mechanisms of WNK1 and WNK4 interaction in the regulation of thiazide-sensitive NaCl cotransport. *J Clin Invest* **115**, 1379–1387.

Acknowledgements

This work was supported National Institute of Dental and Craniofacial Research (NIDCR) grants DE12309 and DK38938, NIH grant GM53032, a Cystic Fibrosis Foundation grant MUALLE05G0, and by the Ruth S. Harrell Professorship in Medical Research.